International Journal of Science and Research Archive
eISSN: 2582-8185
Cross Ref DOI: 10.30574/ijsra
Journal homepage: https://ijsra.net/

(RESEARCH ARTICLE)

Check for updates

COST-EFFECTIVENESS AND OPTIMAL CONTROL ANALYSIS OF MALARIA-TYPHOID CO-INFECTION DYNAMICS AMONG POPULATION SETTINGS IN IDAH

Abu Onoja [1,*] and John Idakwoji A. [2]

[1] Department of Mathematics and Statistics, Federal Polytechnic, Idah, Kogi State, Nigeria.
[2] Department of Science Laboratory Technology, Federal Polytechnic, Idah, Kogi State, Nigeria.
* Corresponding Author

International Journal of Science and Research Archive, 2026, 20(02), 719–734

Publication history: Received on 08 July 2026; revised on 17 August 2026; accepted on 19 August 2026

Article DOI: https://doi.org/10.30574/ijsra.2026.20.2.1637

ABSTRACT

Malaria and typhoid fever are important causes of febrile illness in sub-Saharan Africa, where overlapping clinical manifestations complicate diagnosis, treatment and disease control. This study integrates diagnostic evaluation, mathematical modelling, optimal control and cost-effectiveness analysis to examine malaria–typhoid co-infection in Idah population settings, Kogi State, Nigeria. A diagnostic dataset of 1,000 febrile patients was analysed using expert microscopy/PCR as the malaria reference standard and blood culture with compatible clinical presentation as the typhoid reference standard. Malaria prevalence was 42% and typhoid prevalence was 18%. Malaria RDT recorded 94.05% sensitivity, 91.03% specificity and 92.30% accuracy, while microscopy recorded 90.00%, 97.07% and 94.10%, respectively. For typhoid, Widal test sensitivity, specificity and accuracy were 76.11%, 68.05% and 69.50%; corresponding values for blood culture were 65.00%, 99.02% and 92.90%, and stool culture 57.78%, 98.05% and 90.80%. A deterministic malaria–typhoid co-infection model incorporating environmental transmission and diagnostic error was formulated. Five controls—vector control, improved malaria diagnosis, improved typhoid diagnosis, treatment and environmental sanitation—were evaluated using Pontryagin's Maximum Principle and fourth-order Runge–Kutta simulation over 365 days. Among the fixed intervention strategies, the combined application of all five controls was the most cost-effective, with an incremental cost-effectiveness ratio of approximately ₦426.45 per additional burden unit averted and 610,904.77 burden units averted. The numerical optimal-control strategy achieved 570,056.79 burden units averted at an estimated annual cost of ₦1.106 billion and was cost-saving relative to the diagnosis-plus-treatment strategy. The findings support integrated diagnostic, treatment, vector and environmental interventions as an economically efficient approach to controlling malaria–typhoid co-infection.

Keywords: Malaria; Typhoid Fever; Co-Infection; Diagnostic Accuracy; Optimal Control; Cost-Effectiveness; Mathematical Modelling; Idah

1 INTRODUCTION

Malaria and typhoid fever remain important causes of febrile illness in sub-Saharan Africa, where their geographical and clinical overlap may complicate diagnosis and treatment. Malaria, caused by *Plasmodium* parasites and transmitted mainly by infected female *Anopheles* mosquitoes, continues to account for a substantial proportion of the global malaria

burden, with the African Region carrying most cases and deaths (World Health Organization [WHO], 2025a). Typhoid fever, caused by *Salmonella enterica* serovar Typhi, is primarily transmitted through contaminated food and water and is strongly associated with inadequate sanitation, unsafe water and poor hygiene (WHO, 2023). In communities where both infections occur, patients may present with similar symptoms, increasing the likelihood of diagnostic uncertainty, inappropriate treatment and delayed management.

Reliable laboratory diagnosis is therefore important for effective disease control. WHO recommends parasite-based confirmation of suspected malaria using microscopy or rapid diagnostic tests (RDTs), particularly where clinical symptoms alone cannot reliably distinguish malaria from other febrile illnesses (WHO, 2025b). Although RDTs provide rapid diagnosis, microscopy can offer greater specificity and information on parasite density. For typhoid fever, blood culture remains an important confirmatory method, although its sensitivity may be reduced by prior antibiotic use, low-level bacteraemia and other clinical and laboratory factors (Antillon et al., 2018). The Widal test remains widely used in many resource-limited settings, but its diagnostic reliability is affected by previous exposure, background antibody titres and cross-reactivity. Evidence from endemic settings has demonstrated considerable limitations and variability in the diagnostic performance of the Widal test, including relatively poor specificity and positive predictive value (Muhie et al., 2023).

The simultaneous occurrence of malaria and typhoid fever presents an additional challenge because co-infected patients may require different diagnostic and therapeutic considerations. Evidence from Nigerian populations indicates that malaria–typhoid co-infection remains a relevant clinical problem (Olowolafe et al., 2024). Mathematical modelling provides a useful framework for examining such interacting infections because it permits the transmission processes, disease progression and intervention effects to be investigated simultaneously. Recent malaria–typhoid models have incorporated environmental transmission and co-infection compartments, highlighting the importance of considering the distinct transmission mechanisms of the two diseases (Abah et al., 2025; Uyi-Osagie et al., 2026).

Optimal-control modelling extends this approach by determining how intervention intensity can be varied over time to reduce disease burden while accounting for intervention costs. Previous studies have demonstrated the usefulness of optimal-control and cost-effectiveness methods for comparing malaria interventions, including vector control and treatment (Siva and Torres (2013)). However, relatively few studies have jointly incorporated diagnostic accuracy, malaria transmission, environmental typhoid transmission, co-infection, intervention controls and economic considerations within a single framework.

This study addresses this gap by integrating diagnostic evaluation with a deterministic malaria–typhoid co-infection model for Idah population settings, Kogi State, Nigeria. The study evaluates malaria RDT, microscopy, Widal test, blood culture and stool culture using a diagnostic dataset of 1,000 febrile patients. It then formulates an optimal-control model incorporating vector control, improved malaria diagnosis, improved typhoid diagnosis, treatment and environmental sanitation. Pontryagin's Maximum Principle is used to derive the optimality system, while numerical simulation is employed to compare single and combined control strategies. Cost-effectiveness analysis is subsequently used to identify strategies that provide substantial reductions in malaria, typhoid and co-infection burden at comparatively reasonable intervention costs. The study is intended to provide a quantitative basis for selecting integrated and sustainable control strategies for malaria–typhoid co-infection in endemic population settings.

2 MATERIAL AND METHODS

2.1 Study Design and Population

This study employed an integrated diagnostic, mathematical-modelling and cost-effectiveness design. The diagnostic component used a dataset of 1,000 febrile patients in Idah population settings, Kogi State, Nigeria. Participants were aged 1–70 years and presented with febrile illness suggestive of malaria and/or typhoid fever. The mathematical component linked the diagnostic findings with epidemiological and intervention parameters to investigate malaria–typhoid co-infection dynamics and identify optimal control strategies.

2.2 Diagnostic Dataset and Performance Measures

For malaria, expert microscopy/polymerase chain reaction (PCR) was treated as the reference standard. Estimated malaria prevalence was 42% (420 positive; 580 negative). The evaluated methods were HRP2-based rapid diagnostic test (RDT) and microscopy. For typhoid fever, positive blood culture with compatible clinical presentation was used as the reference standard. Estimated prevalence was 18% (180 positive; 820 negative), and the evaluated methods were Widal test, blood culture and stool culture.

Sensitivity, specificity, positive predictive value (PPV), negative predictive value (NPV) and accuracy were calculated from true-positive (TP), false-positive (FP), true-negative (TN) and false-negative (FN) outcomes.

$$Sensitivity = \frac{TP}{TP + FN} \times 100;$$

$$specificity = \frac{TN}{TN + FP} \times 100;$$

$$PPV = \frac{TP}{TP + FP} \times 100;$$

$$NPV = \frac{TN}{TN + FN} \times 100; \; and$$

$$Accuracy = (TP + TN)/(TP + FP + TN + FN) \times 100.$$

The summary of these measures are given in Table.

Table 1: Sensitivity, specificity, positive predictive value (PPV), negative predictive value (NPV) and accuracy

Test	TP	FP	TN	FN	Sens.	Spec.	Accuracy
Malaria RDT	395	52	528	25	94.05	91.03	92.30
Microscopy	378	17	563	42	90.00	97.07	94.10
Widal	137	262	558	43	76.11	68.05	69.50
Blood culture	117	8	812	63	65.00	99.02	92.90
Stool culture	104	16	804	76	57.78	98.05	90.80

2.3 Mathematical Model

A deterministic compartmental model was formulated for malaria–typhoid co-infection. The human population was divided into susceptible, malaria-exposed, malaria-infectious, typhoid-exposed, typhoid-infectious, co-infected and recovered classes, denoted by $S_h, E_m, I_m, E_t, I_t, I_c \; and \; R_h$. The mosquito population comprised susceptible, exposed and infectious classes $S_v, E_v \; and \; I_v$while environmental Salmonella contamination was represented by B. Thus, $N_{\mathrm{h}} = S_h + E_m + I_m + E_t, + I_t + I_c + R_h$ and $N_{\mathrm{v}} = S_v + E_v + I_v$

The controlled human system is written as

system is written as

$$\left.\begin{aligned}
\frac{dS_h}{dt} &= \Lambda_h - (\lambda_m + \lambda_t + \mu_h)S_h + \omega R_h \\
\frac{dE_m}{dt} &= \lambda_m S_h - (\sigma_m + \mu_h)E_m \\
\frac{dI_m}{dt} &= \sigma_m E_m - \left(\tau_m^{"} + \mu_h + \delta_m\right)I_m - \phi\lambda_t I_m \\
\frac{dE_t}{dt} &= \lambda_t S_h + \phi\lambda_t I_m - (\sigma_t + \mu_h)E_t \\
\frac{dI_t}{dt} &= \sigma_t E_t - \left(\tau_t^{"} + \mu_h + \delta_t\right)I_t - \lambda_t I_t \\
\frac{dI_c}{dt} &= \lambda_t I_t + \phi\lambda_t I_m - \left(\tau_c^{"} + \mu_h + \delta_c\right)I_c \\
\frac{dR_h}{dt} &= \tau_m^{"} I_m + \tau_t^{"} I_t + \tau_c^{"} I_c - (\omega + \mu_h)R_h
\end{aligned}\right\} (\mathbf{2.1})$$

The malaria transmission $\lambda_m = \frac{(1-u_1)\alpha\beta_m I_v}{N_h}$, where β_{m} is the malaria transmission coefficient and α is the mosquito biting rate.

The mosquito controlled system is written as

$$\left.\begin{aligned}\frac{dS_v}{dt} &= \Lambda_v(t) - (1-u_1)\lambda_v S_v - \mu_v S_v \\ \frac{dE_v}{dt} &= (1-u_1)\lambda_v S_v - (\sigma_v + \mu_v)E_v \\ \frac{dI_v}{dt} &= \sigma_v E_v - \mu_v I_v\end{aligned}\right\} (\mathbf{2.2})$$

Where mosquito infection $\lambda_v = \frac{(1-u_1)\beta_v(I_m+\eta I_c)}{N_h}$

The seasonal recruitment is $\Lambda_v(t) = \Lambda_0(1 + \varepsilon cos\frac{2\pi t}{365})$

The controlled environmental salmonella is written as

$$\left.\frac{dB}{dt} = \rho_1 I_t + \rho_2 I_c - (\sigma_b + ku_5)B\right\} (\mathbf{2.3}),$$

k measures the effectiveness of sanitation.

The typhoid transmission $\lambda_t = \frac{(1-u_5)\beta_t B}{K+B}$, where β_t is the environmental transmission coefficient and K is the half-saturation constant.

2.4 Control Variables and Optimal-Control Problem

Five time-dependent controls were considered: $u_1(t)$, vector control; $u_2(t)$, improved malaria diagnosis; $u_3(t)$, improved typhoid diagnosis; $u_4(t)$, prompt and effective treatment; and $u_5(t)$, environmental sanitation. Each control satisfies $0 \le u_i(t) \le 1$. The objective was to minimise the combined epidemiological burden, diagnostic error and intervention costs over 365 days:

The objective functional is written as

$$J(u_1,u_2,u_3,u_4,u_5) = \int_0^T [A_1 I_m + A_2 I_t + A_3 I_C + A_4 B + A_5 FP + A_6 FN + A_7 DT + \frac{1}{2}(B_1 u_1 + B_2 u_2 + B_3 u_3 + B_4 u_4 + B_5 u_5)]dt\Big\} \ (\mathbf{3.4})$$

where $A_1 - A_7$ weight the societal costs of infections, contamination, diagnostic errors and delayed treatment and $B_1 - B_5$ weight the implementation costs of each intervention.

2.5 Optimality System and Numerical Solution

Pontryagin's Maximum Principle was used to derive the necessary optimality conditions. Let the adjoint variables corresponding to $(S_h, E_m, I_m, E_t, I_t, I_c, R_h, S_v, E_v, I_v, B)$ be $(\lambda_1, \lambda_2, \lambda_3, \lambda_4, \lambda_5, \lambda_6, \lambda_7, \lambda_8, \lambda_9, \lambda_{10}, \lambda_{11})$.

The Hamiltonian $H = L(X,u,t) + \lambda^{\mathrm{T}} F(X,u,t)$, is given by

$$\begin{aligned}H = {} & A_1 I_m + A_2 I_t + A_3 I_C + A_4 B + A_5 FP + A_6 FN + A_7 DT + \frac{1}{2}\left(B_1 u_1 + B_2 u_2 + B_3 u_3 + B_4 u_4 + B_5 u_5\right) + \lambda_1 \frac{dS_h}{dt} \\ & + \lambda_2 \frac{dSE_m}{dt} + \lambda_3 \frac{dE_m}{dt} + \lambda_4 \frac{dE_t}{dt} + \lambda_5 \frac{dI_t}{dt} + \lambda_6 \frac{dI_c}{dt} + \lambda_7 \frac{dR_h}{dt} + \lambda_8 \frac{dS_v}{dt} + \lambda_9 \frac{dE_v}{dt} + \lambda_{10} \frac{dI_v}{dt} \\ & + \lambda_{11} \frac{dB}{dt}\Big\} \quad (\mathbf{3.5})\end{aligned}$$

According to Pontryagin's Maximum Principle,

$$\frac{d\lambda_i}{dt} = -\frac{\partial H}{\partial x_i},$$

Where $x_i = (S_h, E_m, I_m, E_t, I_t, I_c, R_h, S_v, E_v, I_v, B)$.

Therefore, the adjoint equations were derived as follows.

$$\left.\begin{aligned}
\frac{d\lambda_1}{dt} &= -\frac{\partial H}{\partial S_h} \\
\frac{d\lambda_2}{dt} &= -\frac{\partial H}{\partial E_m} = (\sigma_m + \mu_h)\lambda_2 - \delta_m\lambda_3 \\
\frac{d\lambda_3}{dt} &= -A_1 + \lambda_3\left(\tau_m^{"} + \mu_h + \delta_m + \phi\lambda_t\right) - \lambda_6\phi\lambda_t - \lambda_7\tau_m^{"} - \lambda_9\frac{\partial\lambda_v}{\partial I_m}S_v + \cdots \\
\frac{d\lambda_4}{dt} &= \lambda_4(\mu_h + \delta_t) - \delta_t\lambda_5 \\
\frac{d\lambda_5}{dt} &= -A_2 + \lambda_5\left(\tau_t^{"} + \mu_h + \delta_t - \lambda_m\right) - \lambda_6\lambda_m - \lambda_7\tau_t^{"} - \rho_1\lambda_{11+\cdots} \\
\frac{d\lambda_6}{dt} &= -A_3 + \lambda_6\left(\tau_c^{"} + \mu_h + \delta_c\right) - \lambda_7\tau_c^{"} - \eta\lambda_9\frac{\beta_v S_v}{N_h} - \rho_2\lambda_{11+\cdots} \\
\frac{d\lambda_7}{dt} &= -(\omega + \mu_h)\lambda_7 + \omega\lambda_{11} \\
\frac{d\lambda_8}{dt} &= (1-u_1)\lambda_v(\lambda_8 - \lambda_9) + \mu_v\lambda_8 \\
\frac{d\lambda_9}{dt} &= (\sigma_v + \mu_v)\lambda_9 - \sigma_v\lambda_{10} \\
\frac{d\lambda_{10}}{dt} &= (\lambda_1 - \lambda_2)\frac{(1-u_1)\alpha\beta_m S_h}{N_h} + \mu_v\lambda_{10} \\
\frac{d\lambda_{11}}{dt} &= -A_4 + \lambda_1\frac{\partial\lambda_t}{\partial B}S_h + \lambda_4\frac{\partial\lambda_t}{\partial B}S_h + (\sigma_b + ku_5)\lambda_{11}
\end{aligned}\right\} \quad (\mathbf{3.6})$$

Transversality conditions are given as

$$\lambda_i(T) = 0, i = 1, \ldots, 11\} \quad (\mathbf{3.7})$$

The optimal controls satisfy

$$\frac{\partial H}{\partial u_i} = 0$$

$$\left.\begin{aligned}
u_1^* &= \min\left\{1, \max\left(0, \frac{\varphi_1}{B_1}\right)\right\}, \varphi_1 = (\lambda_8 - \lambda_9)\lambda_v S_v + (\lambda_1 - \lambda_2)\lambda_m S_h \\
u_2^* &= \min\left\{1, \max\left(0, \frac{\varphi_2}{B_2}\right)\right\}, \varphi_2 = \frac{\partial H}{\partial Se_m}\omega_1 + \frac{\partial H}{\partial Sp_m}\omega_2 \\
u_3^* &= \min\left\{1, \max\left(0, \frac{\varphi_3}{B_3}\right)\right\}, \\
u_4^* &= \min\left\{1, \max\left(0, \frac{\omega_5\lambda_3 I_m + \omega_6\lambda_5 I_t + \omega_7\lambda_6 I_c}{B_4}\right)\right\}, \\
u_5^* &= \min\left\{1, \max\left(0, \frac{k\beta\lambda_{11}}{B_5}\right)\right\}
\end{aligned}\right\} \quad (\mathbf{3.8})$$

The state and adjoint equations were solved iteratively using a fourth-order Runge–Kutta (RK4) forward–backward procedure until convergence. For numerical solution, we used the parameter values in the following tables.

2.6 Cost-Effectiveness Analysis

Alternative single and combined strategies were compared using total intervention cost and integrated disease burden averted. The incremental cost-effectiveness ratio (ICER) was calculated as $ICER_{\mathrm{i}} = (C_{\mathrm{i}} - C_{\mathrm{i-1}})/(E_{\mathrm{i}} - E_{\mathrm{i-1}})$, where C denotes cost and E denotes epidemiological benefit. Dominated strategies—those costing more while producing less benefit—were excluded before ICER comparison. The fixed-strategy analysis identified the combined use of all five controls as the most cost-effective strategy, with an ICER of approximately ₦426.45 per additional burden unit averted.

2.7 Control Strategies Evaluated

The numerical simulations compared no control with individual and combined interventions. The principal strategies were: (i) no control; (ii) vector control; (iii) improved malaria diagnosis; (iv) improved typhoid diagnosis; (v) treatment; (vi) sanitation; (vii) vector control plus treatment; (viii) vector control plus sanitation; (ix) diagnosis plus treatment; (x)

vector control plus diagnosis plus treatment; (xi) vector control plus diagnosis plus sanitation; and (xii) all five controls. This design permits comparison of the epidemiological and economic effects of increasing intervention intensity.

2.8 Simulation Outputs

The principal outcomes were the numbers of malaria-infectious individuals, typhoid-infectious individuals, malaria–typhoid co-infected individuals and the total infectious population. These were reported as actual numbers of persons rather than population proportions. The model trajectories were generated over 365 days for each control combination, allowing direct comparison of the timing and magnitude of intervention effects.

2.9 Reproducibility and Interpretation of Scales

The diagnostic analysis and transmission model represent two related but distinct scales. The diagnostic component comprises the supplied 1,000-patient dataset and is used to quantify diagnostic performance and diagnostic error. The dynamic model represents an estimated Idah population of 100,000 persons.

2.10 Decision Rule for Cost-Effectiveness

Cost-effectiveness was assessed after ordering feasible strategies by increasing effectiveness and removing strictly dominated alternatives. Incremental costs were then compared with incremental burden averted. A lower ICER indicates a more favourable additional cost per unit of epidemiological benefit. The analysis therefore distinguishes the strategy that produces the greatest epidemiological reduction from the strategy that provides the most favourable incremental economic value.

3 RESULTS

3.1 Diagnostic Performance of Malaria and Typhoid Tests

The diagnostic analysis of the 1,000 febrile patients demonstrated appreciable differences among the evaluated methods. For malaria, the HRP2-based rapid diagnostic test (RDT) identified 395 of the 420 reference-standard positive cases and 528 of 580 reference-standard negative cases, achieving 94.05% sensitivity, 91.03% specificity and 92.30% accuracy. Microscopy detected 378 positive cases and correctly classified 563 negative cases, giving 90.00% sensitivity, 97.07% specificity and 94.10% accuracy. Thus, RDT provided higher sensitivity, whereas microscopy provided higher specificity and overall accuracy.

For typhoid fever, the Widal test produced 137 true-positive and 262 false-positive results, corresponding to 76.11% sensitivity, 68.05% specificity and 69.50% accuracy. Blood culture produced only 8 false-positive results and achieved 99.02% specificity and 92.90% accuracy, although sensitivity was 65.00%. Stool culture also demonstrated high specificity (98.05%) but lower sensitivity (57.78%). The high false-positive rate of Widal testing could therefore lead to unnecessary treatment of patients without confirmed typhoid fever.

These findings are epidemiologically important because false-positive and false-negative classifications influence the transmission model through inappropriate treatment, delayed treatment and intervention costs. The relatively high sensitivity of malaria RDT makes it useful for rapid case detection, whereas microscopy provides a confirmatory advantage through greater specificity. For typhoid fever, the higher specificity of culture-based methods supports their use where laboratory capacity permits.

3.2 Numerical Simulation of Malaria–Typhoid Co-Infection

The numerical solution of the optimality system demonstrated clear differences among intervention strategies over the 365-day simulation period. Trajectories were expressed as actual numbers of persons rather than population proportions, using the 100,000-person model population. The no-control scenario provided the baseline. Without intervention, malaria, typhoid and co-infection persisted because transmission through mosquitoes and environmental contamination continued. Individual controls reduced disease burden to varying degrees, while combined interventions generally produced greater reductions in infectious and co-infected populations.

This result is epidemiologically plausible because malaria and typhoid have different principal transmission pathways. Vector control primarily affects malaria transmission, whereas sanitation acts principally through reduction of environmental Salmonella contamination. Diagnosis and treatment influence infectious duration and the consequences of diagnostic error and therefore complement transmission-oriented interventions.

3.3 Effect of Control Strategies on Co-Infection

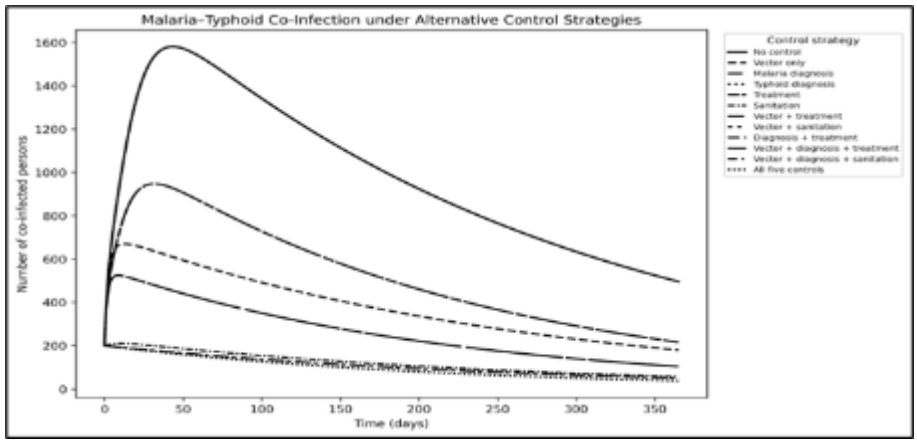

Figure 1: Numerical simulation of the malaria–typhoid co-infected population under alternative control strategies.

Figure 1 presents the malaria–typhoid co-infected population under alternative control strategies. The co-infected population declined more rapidly when interventions were combined than when individual controls were used. The strongest reductions were associated with strategies incorporating several complementary controls. Controlling only one infection does not necessarily eliminate conditions supporting the other; hence vector control alone cannot adequately address environmental typhoid transmission, while sanitation alone cannot sufficiently suppress mosquito-borne malaria.

The importance of combined intervention is consistent with previous malaria optimal-control studies showing that combinations of preventive and therapeutic interventions can outperform isolated strategies when their effects act through different transmission pathways (Silva and Torres (2013)).

3.4 Effect on the Total Infectious Population

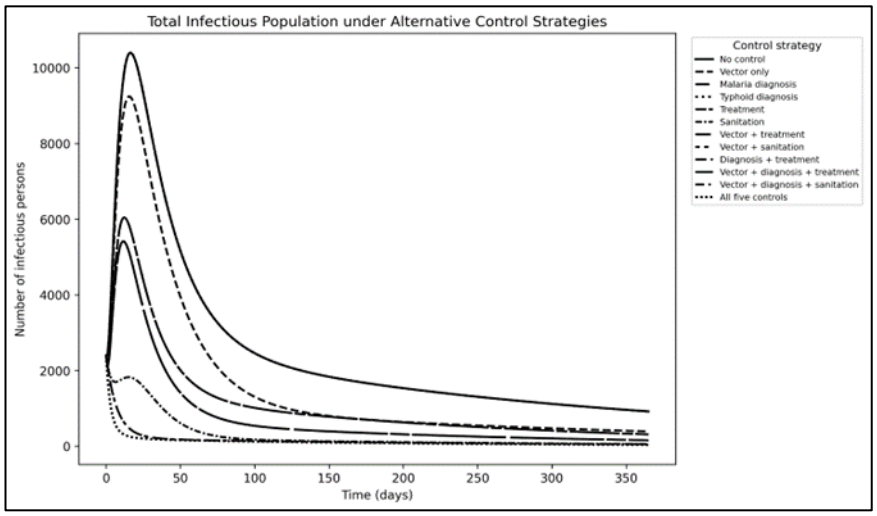

Figure 2: Numerical simulation of the total infectious population under alternative control strategies.

Figure 2 shows the simulated total infectious population, defined as malaria-infectious, typhoid-infectious and co-infected individuals. The no-control trajectory maintained the greatest infectious burden, whereas combined control strategies generated progressively greater reductions. Treatment reduced infectious duration; improved diagnosis increased the likelihood of appropriate treatment while reducing unnecessary treatment; vector control reduced new malaria infections; and sanitation reduced environmental typhoid transmission.

The combined effect is important because reducing one infectious class can indirectly reduce the population entering the co-infected class. Interventions should therefore be evaluated not only according to their direct effect on one disease compartment but also according to their indirect effects on co-infection and the wider infectious population.

3.5 Malaria and Typhoid Infectious Populations

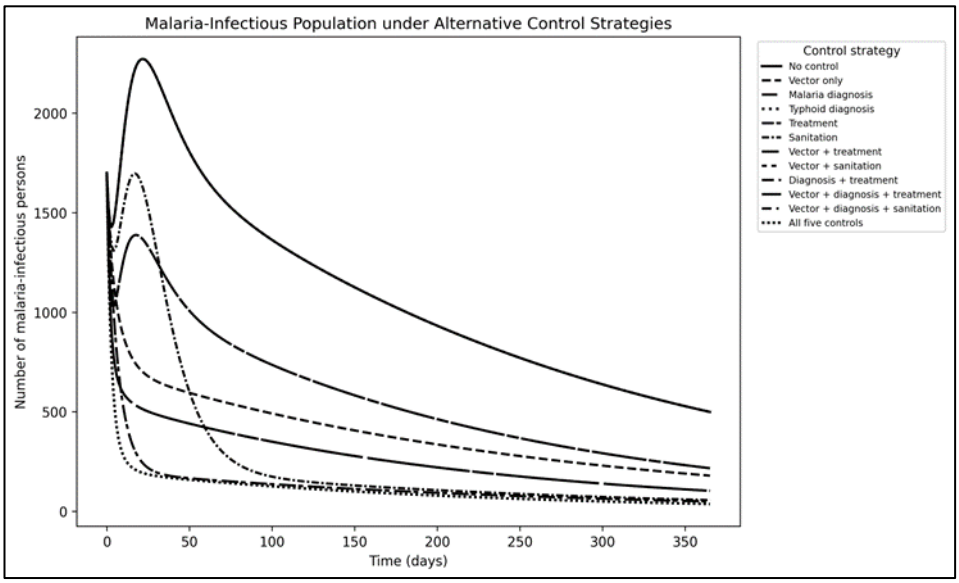

Figure 3: Numerical simulation of the malaria-infectious population under alternative control strategies.

Figure 3 presents malaria-infectious individuals under the alternative strategies. Strategies containing vector control produced pronounced reductions in malaria transmission because they directly reduce mosquito-mediated infection. Diagnosis and treatment further reduced the infectious pool by identifying and treating cases.

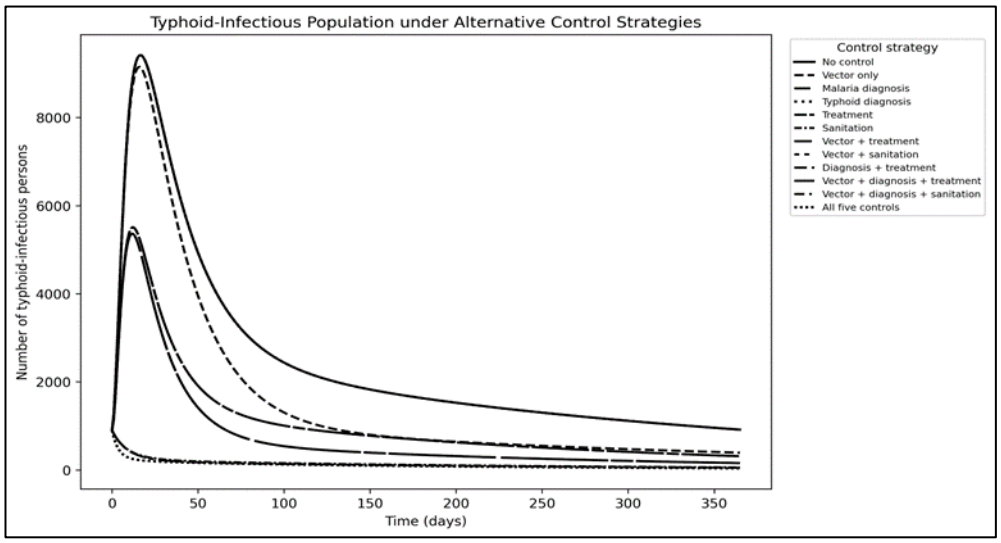

Figure 4: Numerical simulation of the typhoid-infectious population under alternative control strategies.

Figure 4 presents the corresponding typhoid-infectious population. The trajectories demonstrate the importance of sanitation and appropriate diagnosis and treatment. Because the model incorporates environmental Salmonella contamination, sanitation reduces transmission by reducing the environmental reservoir from which new infections arise. The different responses reinforce the rationale for integrated control: mosquito control alone cannot adequately address environmental typhoid transmission, while sanitation alone cannot sufficiently control malaria.

3.6 Comparison of Control Strategies

Twelve strategies were simulated: (1) no control; (2) vector control; (3) improved malaria diagnosis; (4) improved typhoid diagnosis; (5) treatment; (6) sanitation; (7) vector control + treatment; (8) vector control + sanitation; (9) diagnosis + treatment; (10) vector control + diagnosis + treatment; (11) vector control + diagnosis + sanitation; and (12) all five controls.

Strategies involving multiple complementary controls were more effective than most single-control strategies. In particular, the all-five-control strategy simultaneously addressed mosquito transmission, diagnostic error, infectious

duration and environmental contamination. The result also demonstrates that diagnosis should not be considered separately from treatment: improved diagnosis without adequate treatment capacity may identify cases without sufficiently reducing infectious duration, while treatment without reliable diagnosis may result in unnecessary medication and continued diagnostic error.

Table 2: Estimated Disease Burden Weights

Parameter	interpretation	Estimated value
A_1	Cost of one malaria case	50
A_2	Cost of one typhoid case	70
A_3	Cost of one typhoid-malaria case	150
A_4	Environmental salmonella concentration	20
A_5	False positive diagnosis	30
A_6	False negative diagnosis	120
A_7	Delayed treatment	100

Table 3: Estimated Intervention Cost Weights

Parameter	interpretation	Estimated value
B_1	Vector control	600
B_2	Malaria diagnosis (RDT & Microscopy)	300
B_3	Typhoid diagnosis (Widal, stool and blood cultures)	700
B_4	Treatment	450
B_5	Environmental Sanitation	800

Table 4: Human Demographic and Epidemiological Parameters used in Malaria-Typhoid Co-infection Model

Symbol	Description	Baseline value	Unit	Source
Λ_h	Human recruitment rate	20	Persons day^{-1}	Assumed from demographic equilibrium
μ_h	*Natural human mortality rate*	4.6×10^{-5}	day^{-1}	WHO (2024); World Bank (Life expectancy ≈ 60
β_m	Malaria transmission probability per infectious mosquito bite	0.32	day^{-1}	Chitnis et al (2008); Smith et al (2012)
α	Mosquito biting rate	0.30	Bite mosquito^{-1} day^{-1}	Smith et al (2012); WHO (2024)
σ_m	Progression rate from exposed to infectious malaria	0.143	day^{-1}	Incubation period of 7 days; WHO (2024)
$\tau_m^{"}$	Malaria treatment rate	0.20	day^{-1}	Estimated from Nigerian seeking behavior; WHO (2024)
δ_m	Malaria induced mortality rate	0.0010	day^{-1}	WHO (2024)
ω	Loss of acquired immunity	0.0027	day^{-1}	Chitnis et al (2008)
β_t	Typhoid transmission coefficient	0.28	day^{-1}	Calibrated

σ_t	Progression rate from exposed to infectious typhoid	0.071	day^{-1}	Incubation period of 14 days; WHO (2023)
$\tau_t^{"}$	Typhoid treatment rate	0.143	day^{-1}	Average treatment delay ≈ 7 $days$
δ_t	Typhoid induced mortality rate	0.0010	day^{-1}	WHO (2023)
$\tau_c^{"}$	Treatment rate of malaria-typhoid co-infected individual	0.0008	day^{-1}	WHO (2023)
ϕ	Increased susceptibility to typhoid among malaria infected individuals	1.50	dimensionless	Estimated from immunological interaction studies
δ_c	Disease-induced mortality rate due to co-infection	0.0030	day^{-1}	Assumed
Ω	Relative infectiousness of co-infected humans to mosquitoes	1.20	dimensionless	Assumed sensitivity analysis
ρ	Recovery rate after successful treatment	0.143	day^{-1}	WHO (2024)
$N_h(0)$	Initial Human Population	100,000	Persons	Idah LGA Population estimate. National Population Commission

Table 5: Mosquito Population and Environmental Salmonella Parameters

Symbol	Description	Baseline value	Unit	Source
Λ_v	Mosquito recruitment rate	150	Mosquitoes day^{-1}	Chitnis et al (2008)
μ_v	Natural mosquito mortality rate	0.071	day^{-1}	WHO (2024); average life span ≈≈ 14 $days$
β_v	Probability that a susceptible mosquito becomes infected after biting an infectious human	0.25	day^{-1}	Chitnis et al (2008); Chitnis et al. (2012)
σ_v	Mosquito incubation rate	0.100	day^{-1}	WHO (2024); extrinsic incubation rate ≈ 10 $days$
α	Mosquito biting rate	0.30	Bite mosquito^{-1} day^{-1}	Chitnis et al. (2012)
ϵ	Seasonal mosquito recruitment amplitude	0.35	dimensionless	Estimated from Nigerian rainfall seasonality
Λ_0	Average mosquito recruitment	150	mosquitoes^{-1} day^{-1}	calibrated
$N_v(0)$	Initial mosquito population	50,000	mosquitoes	Assumed for simulation
ρ_1	Salmonella shedding rate from infectious typhoid patients	8.0	$CFUL^{-1}day^{-1}$	Assumed
ρ_2	Salmonella shedding rate from infectious malaria-typhoid co-infected patients	12.0	$CFUL^{-1}day^{-1}$	Assumed
δ_b	Natural decay rate of environmental salmonella	0.25	day^{-1}	Assumed

K	Half-saturation constant for environmental transmission	100	$CFUL^{-1}$	Brouwer et al. (2022)
$B(0)$	Initial environmental salmonella concentration	50	$CFUL^{-1}$	Assumed
k	Effectiveness environmental sanitation	0.60	dimensionless	Estimated WHO WASH intervention studies
Ψ	Environmental concentration coefficient	0.40	day^{-1}	Estimated
ε_b	Environmental cleaning efficiency	0.50	Dimensionless	Assumed
θ	Fraction of untreated patients contaminating the environment	0.75	Dimensionless	Estimated
ω_b	Rate of bacterial removal due to chlorination/sanitation	0.30	day^{-1}	WHO WASH Guidelines

Table 6: Diagnostic Test Parameters for Malaria-Typhoid Co-infection Model

Symbol	Description	Baseline value	Unit	Source
Se_{RDT}	Sensitivity of malaria Rapid Diagnostic Test	0.95	Probability	WHO(2024); Okell et al. (2012)
Sp_{RDT}	Specificity of malaria Rapid Diagnostic Test	0.95	Probability	WHO(2024); Okell et al. (2012)
FN_{RDT}	False negativity rate of malaria RDT	0.05	probability	Computed
FP_{RDT}	False positivity rate of RDT	0.05	probability	computed
Se_{mic}	Sensitivity of malaria microscopy	0.90	probability	WHO 2024, Moody (2002)
Sp_{mic}	Specificity of malaria microscopy	0.98	probability	WHO 2024, Moody (2002)
FN_{mic}	False negativity rate of malaria microscopy	0.10	probability	computed
FP_{mic}	False positivity rate of microscopy	0.02	probability	computed
Se_{Wid}	Sensitivity of Widal test	0.74	probability	Parry et al 2002
Sp_{Wid}	Specificity of Widal test	0.68	probability	Parry et al 2002
FN_{Wid}	False negativity rate of Widal test	0.26	probability	computed
FP_{Wid}	False positivity rate of Widal test	0.32	probability	computed
Se_{BC}	Sensitivity of blood culture	0.61	probability	Antillon etal 2018
Sp_{BC}	Specificity of blood culture	1.00	probability	Antillon (2018)
FN_{BC}	False negativity rate of blood culture	0.39	probability	computed
FP_{BC}	False positivity rate of blood culture	0.00	probability	computed
Se_{SC}	Sensitivity of stool culture	0.45	probability	Parry et al 2002
Sp_{SC}	Specificity of stool culture	0.98	probability	WHO (2018)
FN_{SC}	False negative rate of stool culture	0.55	probability	computed
FP_{SC}	False positive rate of stool culture	0.02	probability	computed
ω_1	Effectiveness of improved malaria diagnosis	0.15	Dimensionless	Assumed
ω_2	Effectiveness of improved typhoid diagnosis	0.25	Dimensionless	Assumed

ω_3	Effectiveness of treatment intervention	0.18	Dimensionless	Assumed
ω_4	Effectiveness of vector-control intervention	0.20	Dimensionless	Assumed
ω_5	Fraction of untreated infectious individuals contributing to environmental contamination	0.75	Dimensionless	Assumed
ω_6	Effectiveness of environmental sanitation intervention	0.70	Dimensionless	Assumed
ω_7		0.60		
T	Simulation time horizon	365	Days	One year simulation
C_D	Unit cost of malaria RDT	₦2,000	1 Person	Estimated
C_M	Unit cost of malaria microscopy	₦3,500	1 person	Estimated
C_W	Unit cost of Widal test	₦2,500	1 person	Estimated
C_{BC}	Unit cost of blood culture	₦8,000	1 person	Estimated
C_{SC}	Unit cost of stool culture	₦5,000	1 person	Estimated
C_T	Average treatment cost per malaria case	₦8,500	1 person	Estimated
C_{TY}	Average treatment cost per typhoid case	₦20,000	1 person	Estimated
C_C	Average treatment cost per malaria-typhoid co-infection case	₦35,000	1 person	Estimated
C_V	Annual cost of vector control per protected individual	₦4,500	1 person	Estimated
C_S	Cost of environmental sanitation intervention	₦500,000		Estimated

Table 7: Initial Conditions for Numerical Simulation of the Malaria-Typhoid Model

Symbol	Description	Initial Value	Unit	Source
$S_h(0)$	Initial Susceptible human population	95,000	persons	Assumed based on a population of 100,000
$E_m(0)$	Exposed malaria individuals	500	Persons	Estimated
$I_{m\,(0)}$	Initial infectious malaria individuals	1,500	Persons	Malaria endemic setting estimated
$E_t(0)$	Initial exposed typhoid individuals	300	Persons	Estimated
$I_t(0)$	Initial infectious typhoid individuals	700	Persons	Estimated
$I_c(0)$	Initial malaria-typhoid co-infected individuals	200	Persons	Estimated
$R_h(0)$	Initial recovered individuals	1,800	Persons	Estimated
$N_h(0)$	Total initial human population	100,000	persons	Simulation population
$S_v(0)$	Initial susceptible mosquito population	45,000	Mosquitoes	Assumed
$E_v(0)$	Initial exposed mosquito population	3,000	Mosquitoes	Estimated
$I_v(0)$	Initial infectious mosquito population	2,000	Mosquitoes	Estimated
$N_v(0)$	Total mosquito population	50,000	Mosquitoes	Simulation population
B(0)	Initial environmental salmonella concentration	50	$CFUL^{-1}$	Estimated
$FP_m(0)$	Initial malaria false positive diagnoses	50	Persons	Estimated from diagnostic specificity

$FN_m(0)$	Initial malaria false negative diagnoses	75	Persons	Estimated from diagnostic sensitivity
$FP_t(0)$	Initial typhoid false positive diagnoses	90	Persons	Estimated from diagnostic specificity
$FN_t(0)$	Initial typhoid false negative diagnoses	180	Persons	Estimated from diagnostic sensitivity
MC(0)	Initial missed cases	120	Persons	Estimated
DT(0)	Initial delayed treatment cases	80	Persons	Estimated

Table 8: Control variables

Control	Description	Range
$u_1(t)$	Vector control	$0 \leq u_1 \leq 1$
$u_2(t)$	Improved malaria diagnosis using RDTs and microscopy	$0 \leq u_2 \leq 1$
$u_3(t)$	Improved typhoid diagnosis using Widal test, blood and stool cultures	$0 \leq u_3 \leq 1$
$u_4(t)$	Prompt and effective treatment of malaria, typhoid and co-infected patients	$0 \leq u_4 \leq 1$
u_5(t)	Environmental sanitation to reduce salmonella concentration	$0 \leq u_5 \leq 1$

3.7 Cost-Effectiveness Results

The cost-effectiveness analysis demonstrated that epidemiological effectiveness alone does not determine the preferred intervention. Strategies were compared according to incremental cost and additional disease burden averted after removal of dominated alternatives. Among the fixed intervention strategies, the combined application of all five controls—vector control, improved malaria diagnosis, improved typhoid diagnosis, treatment and environmental sanitation—was identified as the most cost-effective strategy. It produced approximately 610,904.77 burden units averted, with an incremental cost-effectiveness ratio (ICER) of approximately ₦426.45 per additional burden unit averted.

The numerical optimal-control solution produced a complementary result. By allowing control intensities to vary over time rather than applying all interventions at fixed maximum levels, the optimal-control strategy achieved approximately 570,056.79 burden units averted at an estimated annual intervention cost of approximately ₦1.106 billion and was cost-saving relative to the diagnosis-plus-treatment strategy. Thus, the all-five-controls strategy is the most cost-effective fixed strategy, whereas the optimal-control strategy represents a dynamically allocated intervention programme.

4 DISCUSSION

The findings demonstrate that malaria–typhoid co-infection should be addressed as an interacting public-health problem rather than as two completely independent diseases. The diagnostic analysis showed that no single test was optimal across all criteria. The malaria RDT provided high sensitivity, while microscopy achieved greater specificity and accuracy. For typhoid, culture-based methods provided substantially higher specificity than the Widal test. These differences have direct implications for the model because diagnostic errors can alter both estimated disease burden and intervention costs.

The modelling results further demonstrate the value of combining interventions acting at different stages of transmission. Vector control reduces malaria transmission, sanitation reduces environmental typhoid transmission, diagnosis reduces uncertainty and inappropriate treatment, and effective treatment reduces infectious duration. Their combined application consequently produces a broader epidemiological effect than any single intervention.

The cost-effectiveness results show that the all-five-control strategy provides favourable economic value under the assumptions of the model, with an ICER of approximately ₦426.45 per additional burden unit averted. The findings support an integrated malaria–typhoid control strategy combining accurate diagnosis, prompt treatment, vector control and environmental sanitation. The diagnostic dataset and dynamic model represent different scales: the former contains 1,000 febrile patients, while the latter represents a 100,000-person estimated Idah population. Simulated trajectories

should therefore be interpreted as population-level projections rather than observed follow-up outcomes from the diagnostic cohort.

5 CONCLUSION

This study examined malaria–typhoid co-infection through an integrated framework combining diagnostic evaluation, mathematical modelling, optimal control and cost-effectiveness analysis in Idah population setting, Kogi State, Nigeria. The diagnostic analysis showed substantial differences in the performance of the available tests. Malaria RDT demonstrated high sensitivity (94.05%), while microscopy recorded the highest specificity (97.07%) and accuracy (94.10%) among the malaria tests. For typhoid fever, blood culture recorded the highest specificity (99.02%) and accuracy (92.90%), whereas the Widal test showed comparatively poor specificity (68.05%) and the highest false-positive burden.

The mathematical simulations demonstrated that malaria, typhoid and co-infection can persist when transmission is left uncontrolled. Individual interventions reduced disease burden, but combinations of interventions produced greater reductions because they simultaneously addressed the different transmission pathways. Vector control was particularly important for malaria transmission, while environmental sanitation contributed to reducing typhoid transmission through the environmental reservoir. Improved diagnosis and prompt treatment further reduced the infectious population and complemented the preventive interventions.

The cost-effectiveness analysis identified the combined use of all five controls—vector control, improved malaria diagnosis, improved typhoid diagnosis, treatment and environmental sanitation—as the most cost-effective fixed intervention strategy. The strategy produced approximately 610,904.77 burden units averted, with an ICER of approximately ₦426.45 per additional burden unit averted. The numerical optimal-control strategy, which varied intervention intensity over time, provided an alternative economically favourable approach, achieving approximately 570,056.79 burden units averted at an estimated annual intervention cost of ₦1.106 billion and was cost-saving relative to the diagnosis-plus-treatment strategy.

Overall, the findings indicate that malaria–typhoid co-infection requires an integrated rather than disease-specific response. Combining reliable diagnosis, effective treatment, vector control and environmental sanitation offers a more comprehensive approach to reducing transmission, co-infection and associated economic burden. The results provide quantitative support for strengthening integrated febrile-illness management in communities with epidemiological characteristics similar to Idah.

Recommendations

Based on the findings of the study, the following recommendations are made:

- **Integrated control should be prioritised.** Malaria and typhoid control programmes should combine vector control, appropriate diagnosis, effective treatment and environmental sanitation rather than relying predominantly on a single intervention.
- **Diagnostic capacity should be strengthened.** Health facilities should improve access to reliable malaria diagnostic methods, particularly RDTs and microscopy, while culture-based methods should be promoted for confirmation of suspected typhoid fever where laboratory facilities are available.
- **Reliance on Widal testing should be reduced.** The comparatively high false-positive rate observed for the Widal test indicates that it should not be relied upon as the sole basis for confirming typhoid fever, particularly in endemic settings.
- **Prompt and appropriate treatment should accompany diagnosis.** Improving diagnostic accuracy without ensuring timely access to effective treatment would limit the epidemiological benefit of improved case detection.
- **Environmental sanitation should be strengthened.** Provision of safe water, proper waste disposal, improved sanitation facilities and hygiene education should form part of typhoid prevention programmes.
- **Vector-control interventions should be sustained.** Measures that reduce mosquito exposure and transmission should be maintained alongside diagnostic and treatment interventions to suppress malaria transmission.
- **Resources should be allocated using cost-effectiveness evidence.** The all-five-control strategy should be considered when resources permit, given its favourable ICER and substantial disease-burden reduction. Where resources are constrained, the optimal-control framework can assist decision-makers in varying intervention intensity according to epidemiological and economic priorities.
- **Further empirical studies are recommended.** Prospective studies involving larger, directly observed populations in Idah and comparable communities should be undertaken to validate the model assumptions, refine intervention costs and improve the generalisability of the estimated cost-effectiveness outcomes.

STATEMENTS ON COMPLIANCE WITH ETHICAL STANDARDS

Acknowledgments

The authors sincerely appreciate the **Tertiary Education Trust Fund (TETFund), Abuja, Nigeria**, for providing the financial support that facilitated the successful completion of this institution-based research. The authors are grateful for TETFund's continued commitment to promoting research, innovation, and capacity development in Nigerian tertiary institutions.

The authors also express their profound appreciation to the **Management of the Federal Polytechnic, Idah, Kogi State, Nigeria**, for nominating, sponsoring and providing institutional support to the authors to undertake this research. The Management's encouragement, administrative support, and commitment to research development provided an enabling environment for the successful conduct and completion of the study.

The authors further acknowledge all individuals and institutional stakeholders whose contributions, directly or indirectly, supported the development and completion of this work.

Funding Source

This research work was sponsord by TETFunds Insitution Base Research through the Federal Polytechnic, Idah

Disclosure of conflict of interest

The authors declare no conflicts of interest regarding this manuscript.

Statement of ethical approval

Ethical approval was not required for this study as it utilized publicly available, de-identified secondary data. The study protocol complied with institutional and national regulations on the use of secondary data."Statement of Informed Consent:

REFERENCES

[1] Abah, R. T., Agbo, C. E., & Ibrahim, A. (2025). Global stability analysis of a malaria–typhoid fever co-infection model. *FNAS Journal of Mathematical Modeling and Numerical Simulation, 2*(4), 69–84. https://doi.org/10.63561/jmns.v2i4.1125

[2] Antillon, M., Saad, N. J., Baker, S., Pollard, A. J., & Pitzer, V. E. (2018). The relationship between blood sample volume and diagnostic sensitivity of blood culture for typhoid and paratyphoid fever: A systematic review and meta-analysis. *The Journal of Infectious Diseases, 218*(Suppl. 4), S255–S267. https://doi.org/10.1093/infdis/jiy471

[3] Antillon, M., Warren, J. L., Crawford, F. W., Weinberger, D. M., Kürüm, E., Pak, G. D., Marks, F., & Pitzer, V. E. (2017). The burden of typhoid fever in low- and middle-income countries: A meta-regression approach. *PLoS Neglected Tropical Diseases, 11*(2), e0005376. https://doi.org/10.1371/journal.pntd.0005376

[4] Brouwer, A. F., Eisenberg, M. C., Bakker, K. M., Boerger, S. N., Zahid, M. H., Freeman, M. C., & Eisenberg,

[5] Chitnis, N., Hyman, J. M., & Cushing, J. M. (2008). Determining important parameters in the spread of malaria through the sensitivity analysis of a mathematical model. *Bulletin of Mathematical Biology, 70*(5), 1272–1296. https://doi.org/10.1007/s11538-008-9299-0

[6] Chitnis, N., Hardy, D., & Smith, T. (2012). A periodically-forced mathematical model for the seasonal dynamics of malaria in mosquitoes. *Bulletin of Mathematical Biology, 74*, 1098–1124. https://doi.org/10.1007/s11538-011-9710-0

[7] Moody, A. (2002). Rapid diagnostic tests for malaria parasites. *Clinical Microbiology Reviews, 15*(1), 66–78. https://doi.org/10.1128/CMR.15.1.66-78.2002

[8] Muhie, O. A., Abdela, S. G., & Tamirat, K. S. (2023). The accuracy of Widal test for typhoid fever diagnosis in Ethiopia: Systematic review and meta-analysis. *Ethiopian Medical Journal, 61*(2).

[9] Olowolafe, T. A., Agosile, O. F., Akinpelu, A. O., Aderinto, N., Wada, O. Z., & Olawade, D. B. (2024). Malaria and typhoid fever co-infection: A retrospective analysis of University Hospital records in Nigeria. *Malaria Journal, 23*, Article 220. https://doi.org/10.1186/s12936-024-05052-4

[10] Okell, L. C., Bousema, T., Griffin, J. T., Ouédraogo, A. L., Ghani, A. C., & Drakeley, C. J. (2012). Factors determining the occurrence of submicroscopic malaria infections and their relevance for control. *Nature Communications, 3*, Article 1237. https://doi.org/10.1038/ncomms2241

[11] Parry, C. M., Hien, T. T., Dougan, G., White, N. J., & Farrar, J. J. (2002). Typhoid fever. *The New England Journal of Medicine, 347*(22), 1770–1782. https://doi.org/10.1056/NEJMra020201

[12] Silva, C. J., & Torres, D. F. M. (2013). An optimal control approach to malaria prevention via insecticide-treated nets. *Conference Papers in Mathematics, 2013*, Article 658468. https://doi.org/10.1155/2013/658468

[13] Uyi-Osagie, Q., Oduwole, K. H., Umar, M. A., & Audu, A. M. (2026). Mathematical analysis of malaria-typhoid co-infection dynamics with environmental drivers. *The Journals of the Nigerian Association of Mathematical Physics, 71*, 57–72. https://doi.org/10.60787/jnamp.vol71no.607.

[14] World Health Organization. (2023). *Typhoid*. World Health Organization.

[15] World Health Organization. (2024). *[Specific WHO source used for the malaria and typhoid model parameters].* World Health Organization.

[16] World Health Organization. (2025a). *WHO guidelines for malaria*. World Health Organization. https://doi.org/10.2471/B09514

[17] World Health Organization. (2025b). *World malaria report 2025*. World Health Organization. https://doi.org/10.2471/9789240117822

[18] World Bank. (2024). *World development indicators*. World Bank.

[19] National Population Commission. (n.d.). *[Population/census source used for the Idah population estimate].* National Population Commission, Nigeria.